3-2 Emerging Techniques to Enable Asynchronous Coherent OCDMA

WANG Xu, WADA Naoya , and KITAYAMA Ken-ichi

In this paper, we review the recent progress in the key enabling techniques for asynchronous coherent OCDMA: the novel encoder/decoders including spatial lightwave phase modulator, micro-ring resonator for spectral phase coding and superstructured FBG (SSFBG) and AWG type encode/decoder for time-spreading coding; optical thresholding techniques with PPLN and nonlinearity in fiber. The FEC has also been applied in OCDMA system recently.

Most recently, we have demonstrated a record throughput 12×10.71 Gbps truly-asynchronous OCDMA system by using the 16×16 ports AWG-type encoder/decoder and FEC transmit ITU-T G. 709 OTN frames.

1 Background of OCDMA

It is well known that the most critical segment of any telecommunication networks is the last mile because it provides the link to the business and residential customers that can generate the revenues. The next generation last-mile (or access) network, which can deliver next generation services (Ethernet, video and voice) all at the same time, is expected to be a new driving power for telecommunication in the next wave. Only the optical techniques, especially, the passive optical networks (or PON) can provide sufficient bandwidth for this requirement. The existing optical access techniques for this purpose include: time division multiple access (TDMA), wavelength division multiple access (WDMA), sub-carrier multiple access (SCMA), and code division multiple access (CDMA). Figure 1 illustrates the differences of these techniques.

Code division multiple access (CDMA) technique, which has been developed into a great success in wireless communication, enables multiple access communications by assigning unique codes to users[1]. The concept was introduced into fiber optic communication systems in the middle of 80's as optical CDMA (OCDMA), where encoding and decoding operations are all performed in optical domain[2]-[4]. In an OCDMA network, different users are assigned with different codes during transmission. The features and advantages of OCDMA include[4]-[9]:

(1) *All optical processing.* Unlike the wireless CDMA, the coding operations are performed all optically in OCDMA that is desirable for the PON requirement.

(2) *Full asynchronous access.* OCDMA network can work with fully asynchronous access without the requiring of complex and expensive electronic equipment and protocols. This unique advantage of supporting full asynchronous transmission mode makes OCDMA best suited for bursty traffic network.
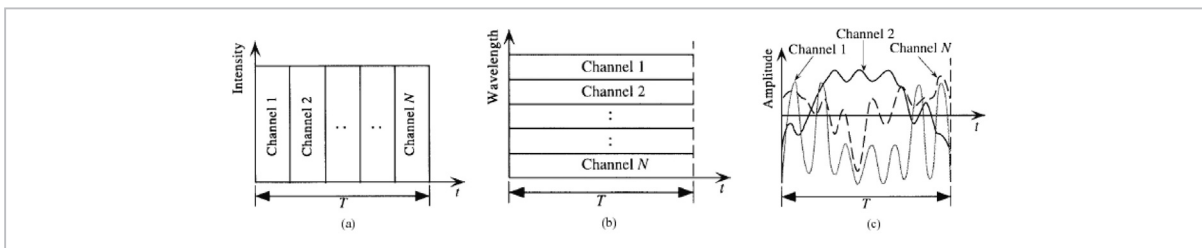
Fig.1 *Illustration of different optical multiple access techniques*
(a) TDMA, (b) WDMA and SCMA, (c) OCDMA

(3) *latency access.* OCDMA could also provide low delay of access as the coding operations are performed all optically and passively.

(4) *Dynamic allocation of bandwidth and soft-capacity-on-demand.* This makes the adding new subscribers or removing unsubscribed users from the network much easy.

(5) *Protocol transparency and decentralized architecture.* The physical layer coding operation guarantees that multiple protocol traffic can be easily supported, while the simple decentralized network architecture simplifies network management.

(6) *Increased flexibility of controlling the Quality of Service (QoS).* QoS guarantees could be managed in physical layer by assigning different code in OCDMA networks.

Therefore, OCDMA is a very promising candidate for next-generation broadband networks and is now receiving increasing interests. Figure 2 shows a basic N×N broadcast OCDMA network architecture, where signal from each transmitter is delivered to every receiver. At each node, it consists of tunable transmitter with a tunable OCDMA encoder and a fixed receiver with a fixed OCDMA decoder followed by electrical integrator and thresholder.

A number of different OCDMA schemes have been proposed, which can be classified by two criteria as illustrated in Fig. 3[9]. The first is by working principle. In *incoherent* OCDMA, the coding is performed on optical power basis, therefore, the OCs are handled in unipolar (0, 1) manner. In *coherent* OCDMA, the coding is performed on field amplitude basis that the OCs are handled in the bipolar (−1, +1) manner all optically. Another is by processing dimensions. The coding can be 1-dimensional (1-D) to be performed in either *time* domain or *frequency* domain, or be 2-dimensional (2-D) to be performed in *frequency* and *time* domains simultaneously.

Devices that have been used as en/decoder for OCDMA include fiber optic delay line (FODL), spatial lightwave modulators (SLM), arrayed-waveguide-grating (AWG), planar
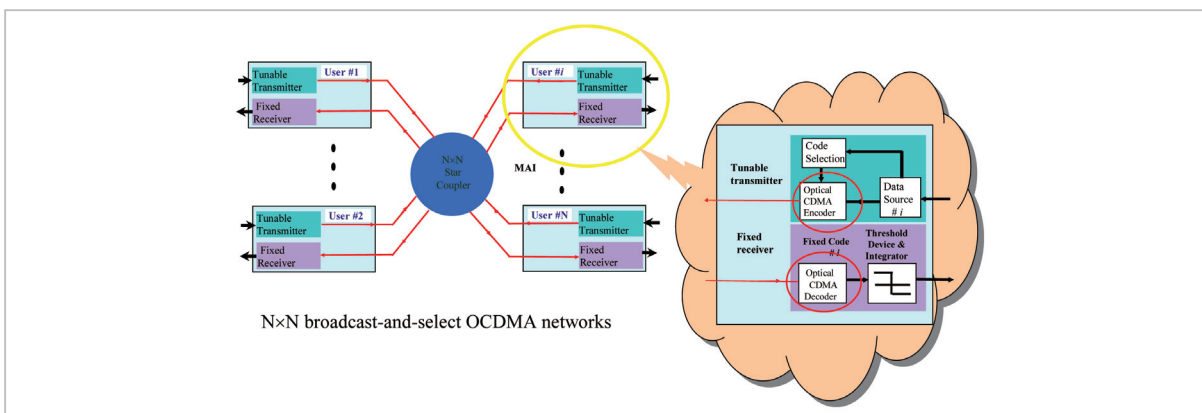
Fig.2 *An example of OCDMA network*
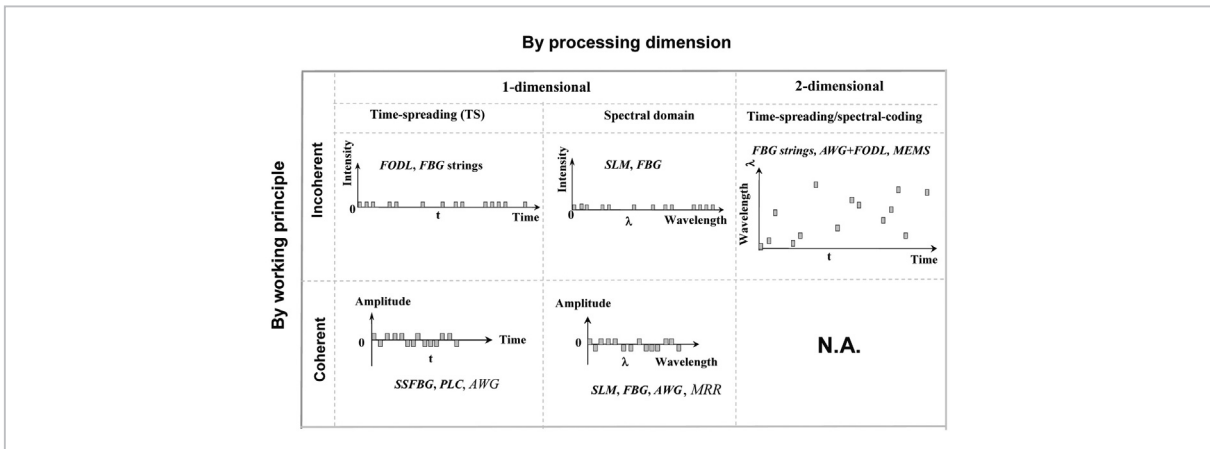
Fig.3 *Classifications of different OCDMA schemes*

lightwave circuits (PLC), fiber-Bragg-gratings (FBG), superstructured FBG (SSFBG), Micro-ring resonator (MRR), and micro-electro-mechanical-systems (MEMS). The using of them in different OCDMA schemes are also indicated in Fig. 3.

2 Key enabling techniques

2.1 En/decoder

(1) SLPM and MRR for high resolution spectral coding

The SPECTS O-CDMA is based on the concept of pulse shaping, where the envelope of a pulse is manipulated by applying different phase shifts to different portions of the pulse's spectrum[17]. Encoding occurs when the applied phase shifts cause a femtosecond pulse to appear as a noise-like burst, and decoding occurs by applying the inverse phase shift to the burst, thereby recovering the original pulse.

Figure 4 shows the configurations and performances of three types of the SLPM developed by different groups. Figure 4(a) is SLPM OCDMA encoder/decoder with the basic configuration using 31-chip M sequences for spectral phase coding, the frequency spacing of different chips is about 75 GHz[19]. Figure 4(b) is the liquid crystal modulator (LCM) based OCDMA encoder/decoder with reflective configuration using 127-chip M sequences for spectral phase coding, the frequency spacing of different chips is about 15 GHz[18]. Figure 4(c) is the configuration of using the Hyperfine optical demultiplexer for OCDMA en/decoding using 16-chip Hadamard codes with chip spacing of about 5 GHz[20].

The above techniques are based on bulk optics, which result in high insertion loss and low compactness. The ultra-compact ring resonator device is ideally suited to this application, providing ultrahigh frequency resolution
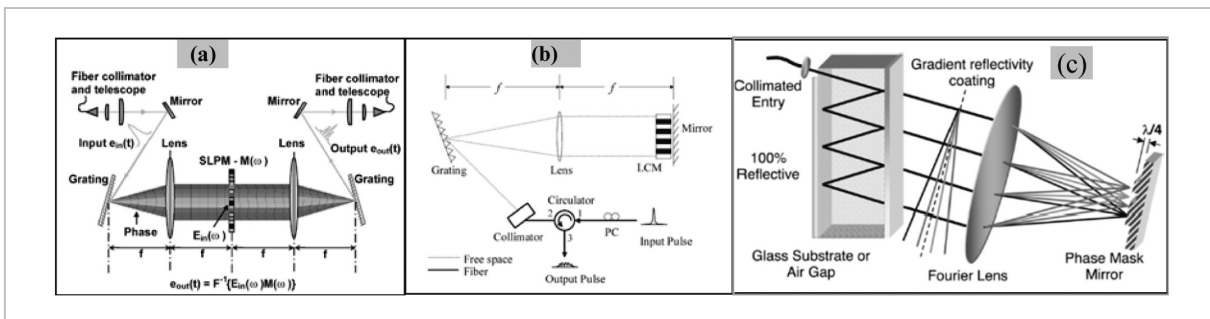
Fig.4 *Configurations and performances of SLPM OCDMA encoder/decoder*

(a) SLPM OCDMA en/decoder[19], (b) LCM-based OCDMA en/decoder[18], (c) Hyperfine optical DMUX for OCDMA[20]

and tuning with programmable, stable, and accurate phase control. The MRR type coder/decoder circuit consists of a common input bus and a common output bus, with 4th order micro ring resonators serving as wavelength selective cross connects between the two as shown in Fig. 5. The ring and bus waveguides were fabricated in the Hydex material system[21], and have a core-to-clad refractive index contrast of 17%. The relative phase shift between two adjacent frequency bins is controlled by a thermo-optic phase heater, shown hatched in Fig. 5. The phase can be continuously varied between 0 and π. The demonstration used 4-chip Hadamad codes with 10 GHz/chip.

All these devices have good tunability that is very flexible for OCDMA application. One issue of the coherent SPECT-OCDMA is the low frequency efficiency. For improving the coding performance and increasing the available codes, longer code is preferable in an OCDMA system, which will need a large number of frequency resources resulting lowered frequency efficiency. To improve this, ultra-high resolution coding devices have to be used to individually control each wave-length line of the ultra-short optical pulses from light source. However, the matching between the wavelength lines of the light source with the passbands of the coding devices is very difficult and results in very stringent stability requirements for both the laser source and the coding devices.

(2) SSFBG and AWG for coherent time spreading

An SSFBG is defined as an FBG with a slowly varying refractive-index modulation profile imposed along its length[12][14]. The full complex refractive-index modulation profile can be realized in an SSFBG by inserting phase shifts between different segments, as shown in Fig. 6(a). With an injection of a short optical pulse, this phase-shifted SSFBG can generate a series of coherent short optical pulses whose phases are determined by the pattern of the phase shifts in the SSFBG. If the refractive-index modulation is constant along the whole grating, the light can penetrate the whole grating length, and the individual segments of the grating contribute more or less equally to the reflected response. The phase-shifted SSFBG thus works as an optical transversal filter to generate a binary-phase-shift-
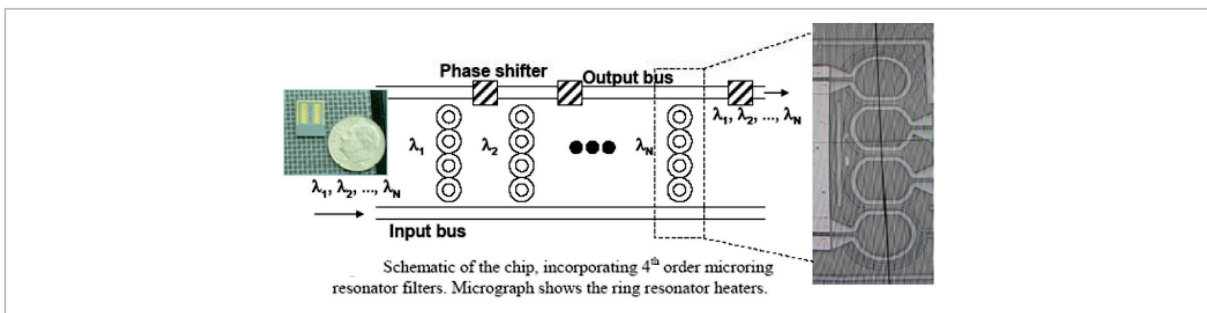
Fig.5 MRR type SPECT OCDMA encode/decoder
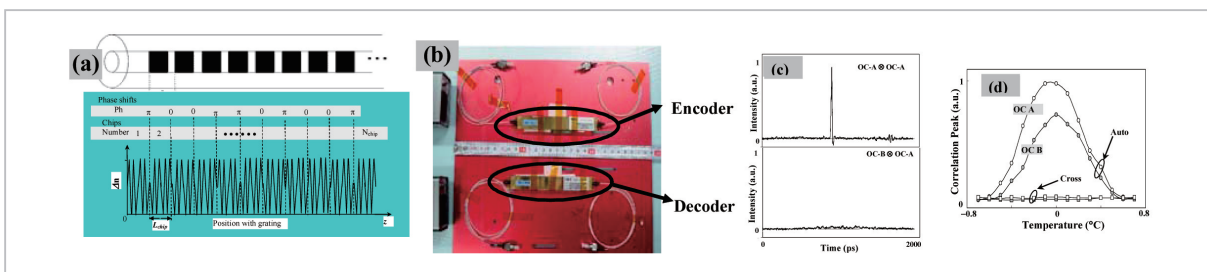
Fig.6 Phase-shifted SSFBG OCDMA encoder/decoder for ultra-long optical code processing

(a) The schematic configuration, (b) Photo of 511-chip SSFBG, (c) Auto-/cross-correlations, (d) Coding performance vs. temperature

key (BPSK)[12] or a quaternary-phase-shift-key (QPSK)[13] optical code from its impulse response, and it can also perform correlation for code recognition. This sort of phase-shifted SSFBG can be fabricated with a single short phase mask by continuous grating writing[12] or holographic techniques[15]. These techniques provide a high flexibility in producing different ultra-long optical code. High-precision phase control can be achieved as well for BPSK, QPSK or even more multiple phase level optical code.

SSFBG encoder/decoder exhibits advantages such as the capability to generate ultra-long optical code with ultra-high chip rate, polarization independent performance, low and code-length independent insertion loss, inherent compatibility with fiber-optic system, high compactness as well as low cost. Figure 6 (b) shows the record-long 511-chip, 640 Gchip/s SSFBG[15][16]. The chip length and the total length of the gratings were 0.156 mm and 80 mm, respectively, which corresponds to a chip rate of 640-Gchip/s with the generated optical code of about 800 ps. The SSFBG was fabricated by using the holographic technique. The central wavelength was 1550 nm at 25°C. Figure 6(c) shows the auto-/cross-correlations, which exhibits very high contrast ratio. The SSFBG central wavelength can be shifted by environmental temperature. Figure 6(d) shows the impact of the temperature variation to the auto-/cross-correlation peaks. The temperature deviation tolerance was ±0.3°C for OC-A, which is still within the temperature stability range of the package (±0.1°C). Using these ultra-long SSFBG OCDMA encoder/decoders,

truly asynchronous multi-user OCDMA experiment has been demonstrated[16].

Another novel optical code encoder/decoder in an AWG configuration has been proposed originally for optical label processing in an optical packet switching experiment[22][23]. Figure 7(a) shows a schematic diagram of the AWG-based multi-port OCDMA encoder/decoder that is able to simultaneously generate and recognize a set of time-spread optical codes with single device[22]. Figure 7(b) is a photo of a 16×16 ports AWG encoder/decoder. The unique capability of simultaneously processing multiple optical codes with one device makes the AWG encoder/decoder a cost effective device for OCDMA networks to be used in the central office to reduce the number of coding devices. Another attractive feature of the AWG encoder/decoder is that it has very high power contrast ratio (PCR) between auto- and cross-correlation signals compared to other coding devices, such as SLPM and SSFBG. We measured the PCR of the 511-chip, 640 Gchip/s SSFBG and the 16×16 ports, 200 Gchip/s AGW encoder/decoder and the results are shown in Fig. 7(c) and (d), respectively. The AWG encoder/decoder can reach 15–20 dB PCR in most of the cases, while the PCR of the SSFBG is around 1 dB. That means the interference level ξ could be significantly reduced (up to 20 dB) using the AWG decoder with the same length of code. Therefore, this device has the potential to tolerate more active users at a high data rate without the need of optical thresholder in an asynchronous OCDMA network[11].
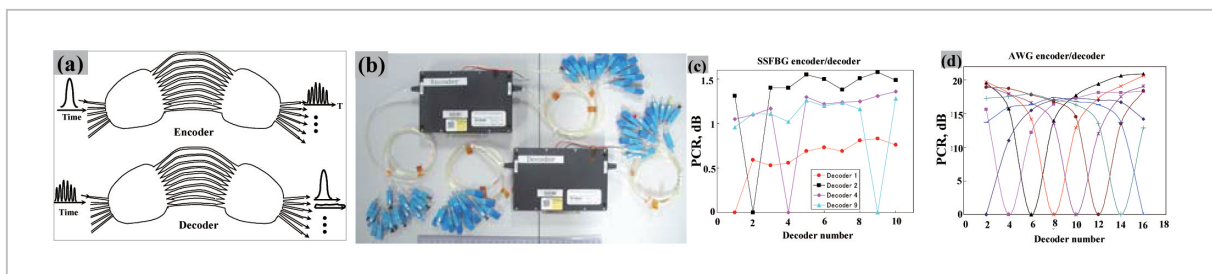
Fig.7 *Coherent time-spreading OCDMA encoder/decoder in an AWG configuration*

(a) Configurations, (b) Photos of 16×16 AWG en/decoder, (c) PCR of 511-chip SSFBG, (d) PCR of the 16×16 AWG en/decoders

2.2 Detection techniques

In an ideal OCDMA network, it is assumed to use chip-rate detection[9]. For coherent TS OCDMA employing long optical code with chip rate as high as several hundreds Gchip/s[14][15], or the coherent spectral coding scheme that employs ultra-short optical pulse[18]-[20], the bandwidth of the receiver can not match the chip-rate detection requirement. Therefore, in a practical system that employs "data-rate" instead of "chip-rate" detection, the MAI noise still remains to be a serious problem. The BER degradation will be resulted due to the receiver's bandwidth limit[9][24]. Using of time gating technique could improve the BER performance by eliminating the MAI noises outside the gating window[25][26], however, strict synchronization (chip level) is needed that makes it not suitable in asynchronous OCDMA. Therefore, applying optical thresholding technique is crucial to enable data-rate detection for achieving a practical asynchronous OCDMA system[9][16][18]-[20].

Several optical thresholding techniques have been applied by using periodically-poled lithium niobate (PPLN)[18] and nonlinear effect in dispersion shifted fiber[27][28], high nonlinear fiber (HNLF)[19], holey fiber[30] and normal dispersion-flattened-fiber (DFF). So far, using the second-harmonic-generation (SHG) in PPLN has achieved the lowest operation power among them. However, the PPLN based device is polarization-dependant that will result in additional polarization mode partition noise in the system. Particularly, this issue could become very severe in an asynchronous OCDMA system since the beat noise is very sensitive to the polarization states of signal[18]. On the contrary, fiber based devices could have less polarization dependency. Nonlinear optical loop mirror (NOLM) was reported to be able to suppress the pedestal of the decoded pulse with low operation power[28], however, it might be not suitable for optical thresholding since the power transfer function of NOLM does not have a steep thrteshold characteristic. While, using self-phase-modulation (SPM) induced signal spectral broadening followed by long-pass-filter[19][27][29] could have better thresholding performance, however, still operate at relatively high power so far. Using super-continuum (SC) generation in normal DFF can be also used for optical thresholding with features the polarization-independency, rather low insertion loss, steep transfer function as well as the pulse reshaping capability[30]. Table I compares the overall performances of different optical thresholding techniques.

Figure 8 (a) shows the configuration and operation principle of the SC-based optical thresholder. It is composed of an EDFA, a 2 km-long DFF, and a 5 nm bandpass filter (BPF). The zero dispersion wavelengths of the fiber are 1523/1575 nm. The operation principle is that: the EDFA boosts the decoded optical signal to a proper level, the correctly decoded pulse, which have a well defined shape with ~2 ps pulsewidth and high peak power, will be able to generate SC in the DFF, while the incorrectly decoded signals (MAI noise) will spread over a large time span with very low peak power that is unable to generate

Table 1 *Performance comparison of different optical thresholding techniques*

Scheme		Data rate	Pulse width	Contrast ratio	Insertion loss	Required power			Polarization	Remarks
						Average	Peak (dBm)	Energy pJ/bit		
Nonlinear effects in fiber	DSF [27]	31.2 MHz	600-800 fs	30 dB	~10dB	0.44 mW	23.5 W	14.1	Independent	
	HNLF [19]	10 G	400 fs	23 dB		25 mW	6.3 W	2.5		
	Holey fiber [29]	1.25 G	2.5 ps		25dB	>2 W	640 W	1600		
	DFF (SC) [30]	1.25G	2 ps	13 dB	13dB	<~ 2mW	~ 6.3 W	12.6		Pulse reshaping
PPLN [18]		10 G	400 fs	20 dB		0.28mW	70 mW	0.03	Dependant	Pulse broadening
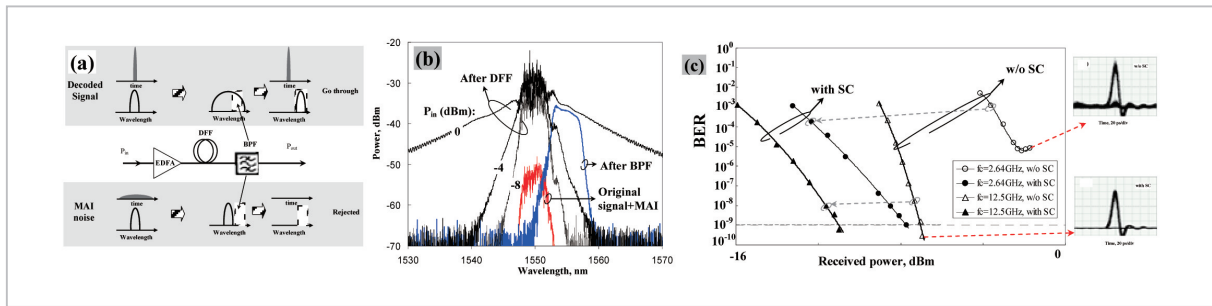
Fig.8 The SC-based optical thresholder using DFF

(a) Configuration and operation principle, (b) Measured spectra, (c) BER performances

SC. The BPF only allows the SC signal passing through and rejects the original signal. Therefore, after BPF, the correctly decoded signal can be recovered without MAI noise. Figure 8(b) shows the measured spectra of the original pulse, generated SC with different input power and signal after BPF. The BER performances and eye diagrams with and w/o SC-based optical thresholder for different receiver bandwidth f_c are shown in Fig. 8(c). The improvement of using optical thresholding to remove MAI noise is significant.

3 Asynchronous multi-user OCDMA experiments

3.1 10-user, Gigabit truly-asynchronous OCDMA experiment

Figure 9 shows the experimental setup of the 10-user asynchronous coherent OCDMA testbed[16]. An optical pulse train with ~1.8 ps pulsewidth was generated by the mode-locked laser diode (MLLD) and modulated by $2^{23}-1$ pseudo-random bit sequence (PRBS) at 1.25 Gbit/s. The amplified signal was equally split into ten arms and encoded by 10 different encoders. The encoders are 511-chip, 640 Gchip/s SSFBGs whose frequency responses are shown in the top-left inset of Fig. 9. Codes 1‒10 are carefully chosen from 511-chip BPSKGold codes so as to have relatively low aperiodic cross-correlations. Fixed fiber delay lines with different lengths are inserted in the ten arms to randomly set the time delays and de-coherence signals of different users. Tunable optical delay lines (DL) are

inserted as well to investigate the impact of different phases of signal-interference overlapping. In a practical PON environment, the polarization states of the signals may be random. However, for investigating the system performance in the worst scenario that the interference becomes most serious, polarization controllers (PC) are placed to align the polarization states of all signals. Besides, tunable attenuators (with switches) are used in all arms to balance the power levels from the 10 users and adjust the number of active users.

The 10-user OCDMA signals are mixed, amplified and launched into 50 km single mode fiber. Dispersion compensation fiber (DCF) is employed to compensate the transmission dispersion. The duration of encoded waveform (~800 ps) is slightly shorter than that of one bit (~804 ps). Therefore, as illustrated in the bottom-right inset of Fig. 10, signal overlaps with interferences completely in this asynchronous experiment, no blank timeslot has been reserved for timing coordination.

At the receiver side, four SSFBG decoders were employed to recover signals from users 1, 2, 4, and 9. In the experiment, we employed the SC-based optical thresholding to eliminate the MAI noise. The average operation power is about 1.4 and 10.3 dBm for K=1 and 10, respectively. In the 10-user experiment, the OCDMA signals were mixed in a truly-asynchronous manner with random time delays, random data patterns, random bit phases, and random polarization states. We have also tested in the worst scenario: bit synchronous and aligned polarization state. In all these cases,
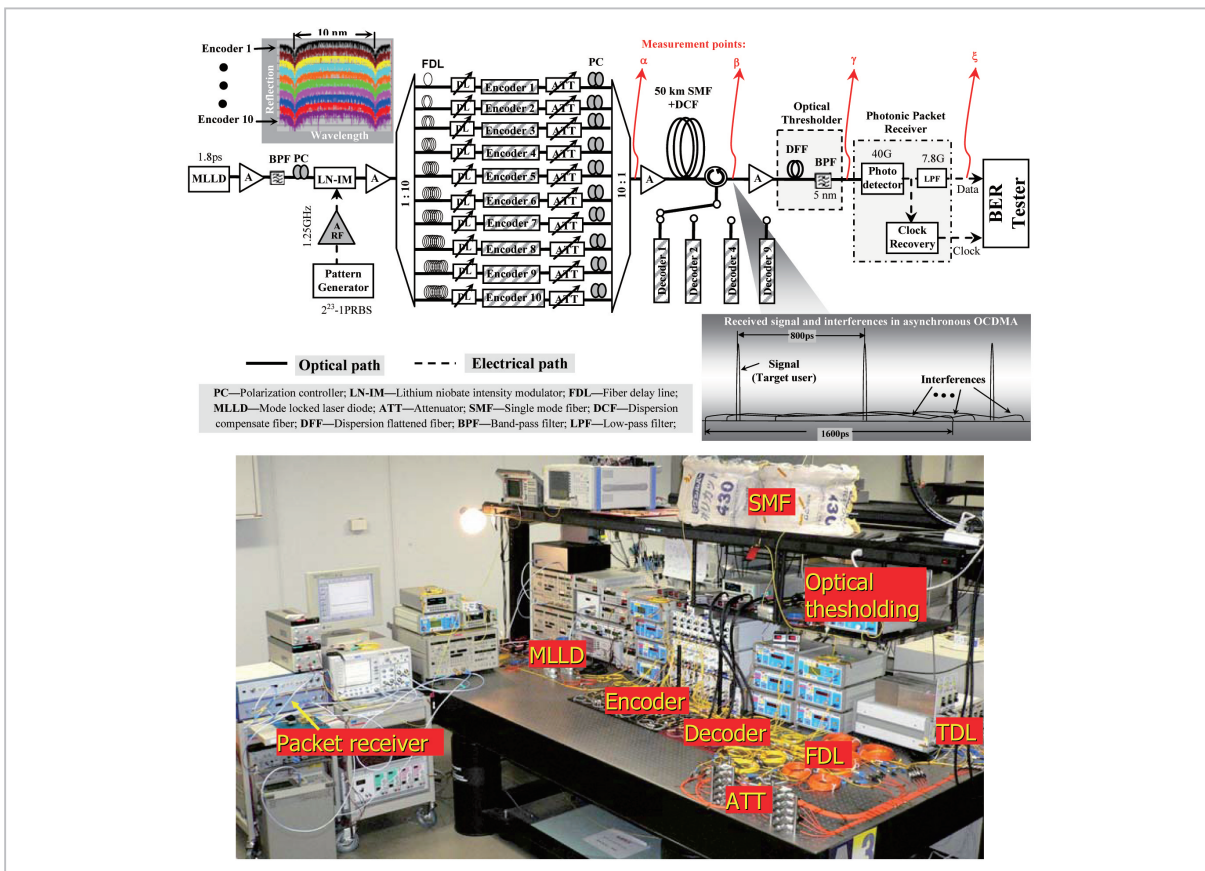
Fig.9 Experimental setup of the 10-user full asynchronous coherent OCDMA testbed

error-free transmission has been achieved for all 4 receivers. This fact confirms that the SI beat noise and the MAI have been suppressed effectively as predicted by the theory.

3.2 12-user, 10.71 Gbps truly asynchronous OCDMA experiment

In this experiment, the 16×16 ports AWG-based OCDMA encoder/decoder with very high PCR was used[11]. Another enabling technique that we used to enhance the performance of an asynchronous OCDMA with MAI and beat noise is FEC[7]. The Reed-Solomon (RS) FEC is very powerful that could improve the BER from 10^{-4} to 10^{-14} with approximately 6 dB net coding gain. The ITU-T G.709 has recommended the interface for optical transmission network (OTN) that consists of RS(253, 239) FEC[31]. Figure 10(a) and (b) show the experimental setup. A 10.71 GHz optical pulse stream was modulated with OTN frame generated by an Anritsu

MP1590B Network Performance Tester. The frame contains $2^{31}-1$ PRBS payload data and FEC parity. The optical signal was forwarded into port #1 of the 16×16 ports, 200 Gchip/s AWG encoder and 16 different OCs have been generated at the 16 output ports; each code is composed of 16 chips. These 16 signals were mixed in a truly-asynchronous manner with balanced power, random delay, random bit phase and random polarization states emulating a 16×10.71 Gbps asynchronous OCDMA network. The OCDMA signal was then boosted and fed into one port of the AWG decoder. The decoded signal from output port 1 was sent for detection. The measured BER performances are shown in Fig. 10(c). In the experiment, we intentionally adjusted the PCs and tunable optical delay lines to test the system performance in the worst-case scenario. Up to K=14 has been achieved error free for decoder port #6. However, the BER performances are not uniform for different users, say for port

(a) Experimental setup

(b) Photo of the 12×10.7 Gbps throughput OCDMA testbed (c) experimental results
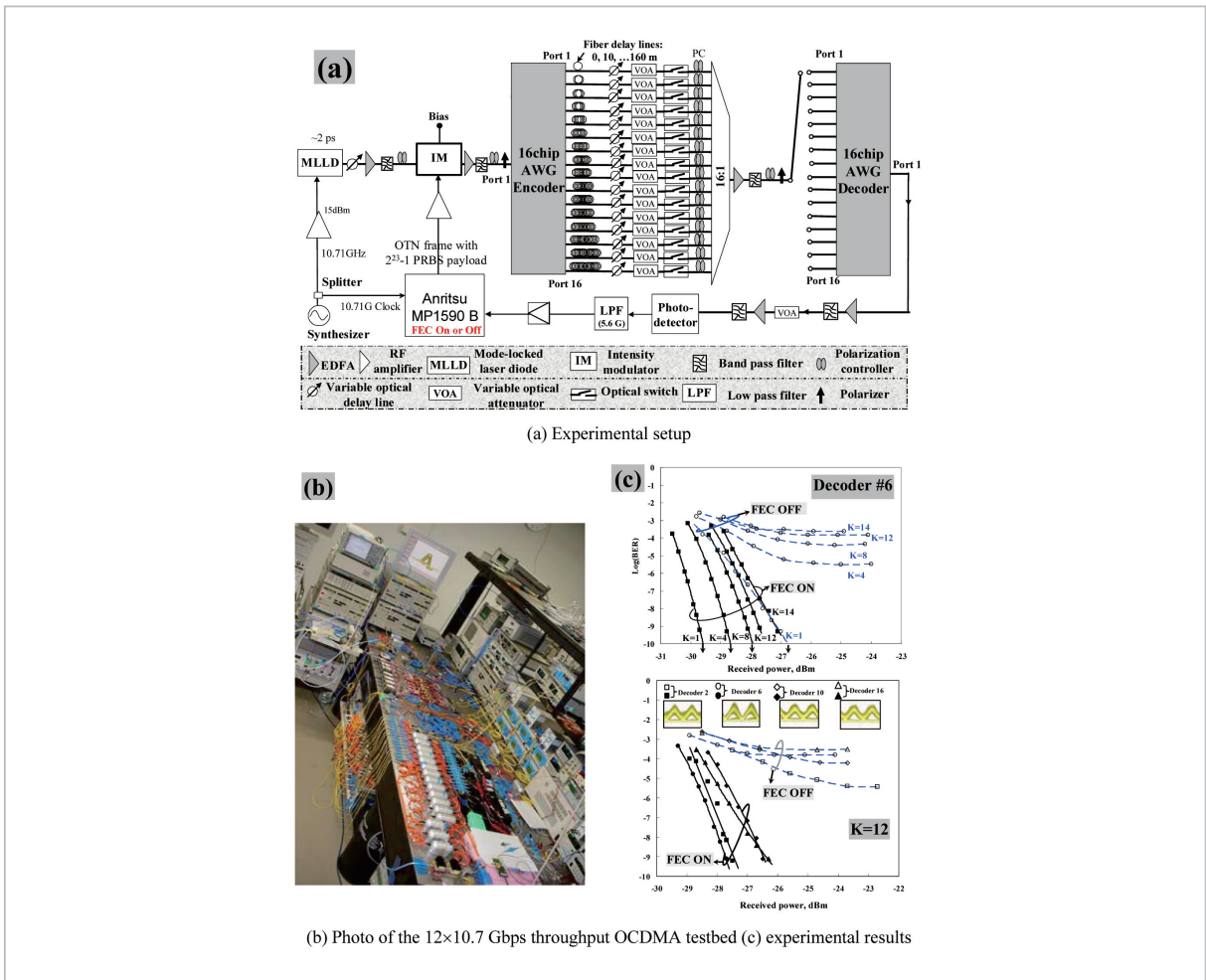
Fig.10 *Demonstration of 12-user, 10.71 Gbps truly asynchronous OCDMA*

#16, which is one of the worst ports, error free could only be achieved for up to K=12. This is mainly due to the non-uniformity of PCR as the result of the fabrication imperfectness of the AWG encoder/decoder. For four different users (decoder ports 2, 6, 10, 16) with K=12, error free has been achieved in all the cases verifying that 12 × 10.71 Gbps throughput asynchronous OCDMA has been successfully demonstrated in the experiment.

4 Conclusions

Having had the mature optical devices and technologies, the OCDMA exhibits a good prospect for practical applications in future broadband access networks.

The key enabling technologies towards practical asynchronous OCDMA networks were discussed in terms of encoder/decoder and optical thresholding. The SSFBG can generate ultra-long OC with low insertion loss. The AWG-type encoder/decoder can process multiple optical codes simultaneously with a single device and have very high PCR that can tolerate more active users at high data-rate. A 10-user truly-asynchronous OCDMA transmission has been demonstrated at 1.25 Gbps with 511-chip SSFBG and SC-based optical thresholder. Most recently, using the 16 × 16 ports AWG-type encoder/decoder, a record throughput 12 × 10.71 Gbps truly-asynchronous OCDMA has been successfully demonstrated to transmit ITU-T G.709 OTN frames. The RS-FEC is another powerful technique to enable this achievement.

References

1 A. J. Viterbi, "CDMA: Principles of Spread Spectrum Communication", Reading, MA: Addison-wesley, 1995.

2 J.Y. Hui, IEEE. J. Slect. Areas in Commun., 3, 916-927, 1985.

3 P. R. Prucnal, M. A. Santoro, and T. R. Fan, J. Lightwave Technol. 4, 547-554, 1986.

4 J. A. Salehi, IEEE Trans. Commun. 37, 824-842, 1989

5 J. A. Salehi, A. M.Weiner, and J. P. Heritage, J. Lightwave Technol., 8, 478-491, 1990.

6 D. D. Sampson, G. J. Pendock, and R. A. Griffin, Fiber and Integrated Optics, 16, 126-157, 1997.

7 K. Kitayama, X. Wang and H. Sotobayashi, ECOC'04, Tu.4.6.1. (invited paper), 2004.

8 A. Stock and E. H. Sargent, IEEE Communication Magazine, 40, 83- 87, 2002.

9 X. Wang and K. Kitayama, IEEE J. Lightwave Technol., 22, 2226-2235, 2004.

10 L. Tancevski and I. Andonovic, Electronics Lett., 30, 1388-1390, 1994.

11 X. Wang, N. Wada, G. Cincotti, T. Miyazaki, and K. Kitayama, ECOC'05 postdeadline, Th4.5.3, 2005.

12 P. C. Teh, P. Petropoulos, M. Ibsen, and D. J. Richardson, J. Lightwave Technol., 9, 1352-1365, 2001.

13 P. C. Teh, M. Ibsen, J. H. Lee, P. Petropoulos, and D. J. Richardson, IEEE Photonic Technol. Lett. 14, 227-229, 2002.

14 Xu Wang, K. Matsushima, A. Nishiki, N. Wada, and K. Kitayama, Optics express, 12, 5457-5468, 2004.

15 X. Wang, K. Matsushima, A. Nishiki, N. Wada, F. Kubota, and K. Kitayama, Optics Lett., 30, 355-357, 2005.

16 X. Wang, N. Wada, T. Hamanaka, and K. Kitayama, OFC'05 postdeadline, PDP 33, 2005.

17 A. M. Weiner, Rev. Sci. Instrum., 71, 1929-1960, 2000.

18 Z. Jiang, D. S. Seo, S.-D. Yang, D. E. Leaird, R. V. Roussev, C. Langrock, M. M. Fejer, and A. M. Weiner, IEEE J. Lightwave Technol., 23, 143-158, 2005.

19 V. J. Hernandez, Y. Du, W. Cong, R. P. Scott, K. Li, J. P. Heritage, Z. Ding, B. H. Kolner, and S. J. Ben Yoo, IEEE J. Lightwave Technol., 22, 2671-2679, 2004.

20 S. Etemad, P. Toliver, R. Menendez, J. Young, T. Banwell, S. Galli, J. Jackel, P. Delfyett, C. Price, and T. Turpin, IEEE Photonic Technol. Lett. 17, 929-931, 2005.

21 A. Agarwal, P. Toliver, R. Menendez, S. Etemad, J. Jackel, J. Young, T. Banwell, B.E. Little, S. T. Chu, and P. Delfyett, OFC'05 postdeadline, PDP 6, 2005.

22 G. Cincotti, IEEE J. Lightwave Technol., 22, 1642-1650, 2004.

23 G. Cincotti, N. Wada, S. Yoshima, N. Kataoka, K. Kitayama, OFC'05 postdeadline, PDP 37, 2005.

24 X. Wang, N. Wada, and K. Kitayama, LEOS 2005, WW2, 2005.

25 P. Petropoulos, N. Wada, P. C. The, M. Ibsen, W. Chujo, K. I. Kitayama, and D. J. Richardson, IEEE Photon. Tech. Lett., 13, 1239-1241, 2001.

26 H. Sotobayashi, W. Chujo, and K. Kitayama, IEEE Photon. Tech. Lett., 14, 555-557, 2002.

27 H. P. Sardesai, and A. M. Weiner, Electron. Lett., 33, 610-611, 1997.

28 J. H. Lee, P. C. Teh, P. Petropoulos, M. Ibsen, and D. J. Richardson, J. Lightwave Technol., 20, 36-46, 2002.

29 J. H. Lee, P. C. Teh, Z. Yusoff, M. Ibsen, W. Belardi, T. M. Monro, and D. J. Richardson, IEEE Photonics Technol. Lett., 14, 876-878, 2002.

30 X. Wang, T. Hamanaka, N. Wada, and K. Kitayama, OSA Optics Express, 13, 5499-5505, 2005.

31 Interfaces for the Optical Transport Network, ITU-T Recommendation G.709/Y.1331, Feb. 2001.

WANG Xu, *Ph.D.*

Limited Term Researcher, Ultrafast Photonic Network Group, New Generation Network Research Center (former: Expert Researcher, Ultrafast Photonic Network Group, Information and Network Systems Department)

Photonic Network

KITAYAMA Ken-ichi, *Dr.Eng.*

Professor, Graduate School of Engineering, Osaka University

Photonic Network

WADA Naoya, *Ph.D.*

Reseaerch Manager, Ultrafast Photonic Network Group, New Generation Network Research Center (former: Senior Researcher, Ultrafast Photonic Network Group, Information and Network Systems Department)

Photonic Network